Thorne, C. P., Wang, C. X. & Carter, J. P. (2004). *Géotechnique* **54**, No. 8, 507–517

Uplift capacity of rapidly loaded strip anchors in uniform strength clay

C. P. THORNE*, C. X. WANG† and J. P. CARTER*

The behaviour of horizontal strip anchors buried in clay is examined in this paper. A brief critique of the various approaches suggested for the design of these anchors is presented, with emphasis placed on estimation of the ultimate load that these anchors can withstand when loaded rapidly in uplift under undrained conditions. Possible mechanisms of failure are reviewed, including shear and tensile failure within the soil and the development of suction within the pore fluid, and the results of finite element predictions are compared with experimental data for ultimate loads. The analyses reveal that the behaviour of strip anchors in uplift is a function of the following non-dimensional parameters: H/B, $\gamma H/c$ and u_c/c, where H is the depth of embedment of the anchor, B is the width of the strip anchor, γ is the unit weight of the soil, c is its undrained shear strength, and u_c is the magnitude of the maximum tensile stress that can be sustained by the pore water in the soil. It is demonstrated that the ultimate uplift capacity is dependent on the availability of water at the surface of the soil and within the soil beneath the strip anchor. The analyses also show that shallow anchors in relatively strong soil tend to fail by the development of tensile failure in the soil above the anchor. The ultimate capacity of these shallow anchors is a function of the undrained shear strength of the soil, its self-weight and the tensile capacity of the pore fluid. By contrast, the failure mechanism for deeply buried anchors where the initial vertical total stress at the plate exceeds $7c$ involves only localised shear failure around the anchor, and as a result the ultimate capacity effectively becomes a function only of the undrained shear strength of the soil.

KEYWORDS: anchors; design; failure; numerical modelling and analysis; plasticity; pore pressures; suction; shear strength

Nous examinons dans cette étude le comportement d'ancres en bande horizontales enfouies dans de l'argile. Nous présentons une brève critique des diverses méthodes suggérées pour la conception de ces ancres, en insistant sur l'estimation de la charge ultime que ces ancres peuvent supporter lorsque ces ancres sont chargées rapidement dans des conditions de redressement non drainées. Nous passons en revue les éventuels mécanismes de défaillance, dont la défaillance de cisaillement et de traction dans le sol et le développement d'une succion dans le fluide interstitiel, et nous comparons les résultats des prédictions d'éléments finis avec les données expérimentales pour des charges ultimes. Les analyses révèlent que le comportement d'ancres en bandes lors du redressement est fonction des paramètres non dimensionnels suivants : H/B, yH/c et u_c/c, H étant la profondeur d'enfouissement de l'ancre, B étant la largeur de l'ancre, y étant le poids unitaire du sol, c étant la résistance de cisaillement non drainé et uc étant la magnitude de l'eau de pore dans le sol. Il est démontré que la capacité de redressement ultime dépend de la disponibilité de l'eau à la surface du sol et à l'intérieur du sol sous l'ancre en bande. Les analyses montrent aussi que les ancres enfouies peu profondément dans des sols relativement forts ont tendance à être déficientes à cause du développement de défaillance de résistance à la traction dans le sol au-dessus de l'ancre. La capacité ultime de ces ancres peu profondes est fonction de la résistance au cisaillement non drainé du sol, de son poids propre et de la capacité de résistance à la traction du fluide de pore. Par contraste, le mécanisme de défaillance pour des ancres enfoncées profondément où la contrainte totale verticale initiale dépasse $7c$ cause uniquement une défaillance de cisaillement localisée autour de l'ancre et en raison de la capacité ultime devient en fait fonction uniquement de la résistance au cisaillement non drainé du sol.

INTRODUCTION

The behaviour of horizontal or near horizontal buried anchors in vertical uplift loading is important to a number of engineering applications, including transmission tower anchors, variable geometry drag anchors, and other forms of marine anchor system. This paper provides a brief critique of the available approaches to the design of these anchors in clay when subjected to rapidly applied uplift loading—that is, under undrained conditions. Shortcomings of the current design methods are identified, and the results of analyses to allow a more rational design approach are provided.

Figure 1 shows the problem investigated and defines the key parameters. Most references (e.g. Meyerhof & Adams,

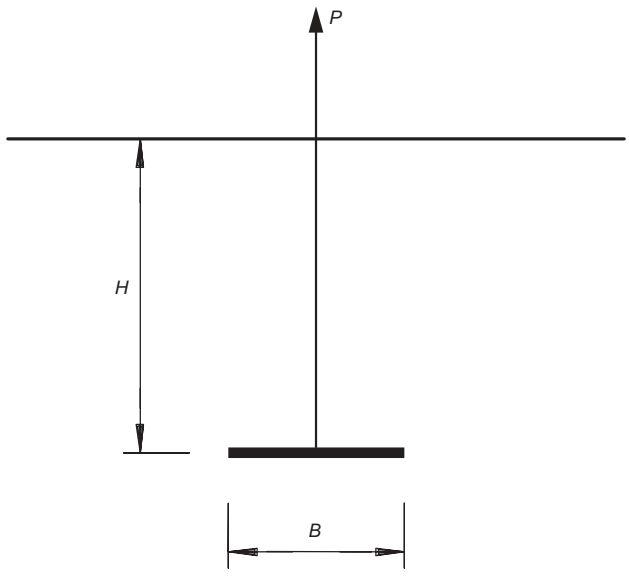

Fig. 1. Uplift of a strip anchor

Manuscript received 10 June 2003; revised manuscript accepted 22 July 2003.
Discussion on this paper closes on 1 May 2005, for further details see p. ii.
* Department of Civil Engineering, The University of Sydney, Australia.
† Faculty of Design, Architecture and Building, The University of Technology Sydney, Australia.

1968; Davie & Sutherland, 1977; Sutherland, 1988) give the ultimate uplift capacity of a strip buried in a uniform cohesive soil and loaded under undrained conditions as

$$P_{ult} = B(Fc + \gamma H) \quad (1)$$

where P_{ult} is the ultimate resistance in uplift per unit length of the strip anchor (kN/m), B is the width of buried strip anchor (m), c is the undrained shear strength of the clay (kPa), F is the uplift capacity factor, H is the depth of the strip below the surface (m), and γ is the total unit weight of soil (kN/m^3). Some references, however, do not include the soil self-weight term (e.g. Das & Singh, 1994; Forrest *et al.*, 1995).

Rowe & Davis (1982) and Merifield *et al.* (1999, 2001) use equation (1) but apply a limiting value for the capacity of a buried strip anchor. That is:

$$P_{ult} = 11{\cdot}42Bc \quad (2)$$

Most of the analytical models in the literature, including the latter two, are based on weightless soil models with the effect of density superimposed. In their study Merifield *et al.* (2001) concluded that the errors incurred by assuming superposition are likely to be relatively insignificant for infinitesimal strain analyses. This paper presents analyses in which the soil density and other factors noted below are included in the initial analyses, i.e. superposition of the self-weight effect is not assumed *a priori*.

In this paper the results are presented for the uplift capacity N_c, defined as

$$P_{ult} = N_c Bc \quad (3)$$

One of the major aims of the paper is to investigate the phenomena of tensile failure in the soil and the development of suction pore water pressures, and the influence they have on the ultimate capacity of strip anchors.

MECHANISMS OF FAILURE

Mechanisms of failure for various conditions

Uplift loading produces different stress changes in various regions of the soil. In the region below the strip anchor there is a reduction in the total vertical stress, whereas in the region immediately above the strip there is an increase in total vertical stress. The surface directly above the strip tends to bulge upwards, with the intervening soil acting as a form of beam. This 'beam' action results in a decrease in the horizontal stress that can lead to tensile stresses. Tensile failure is unusual in soil mechanics, though several authors have noted tensile cracking above the plate during loading in tests (e.g. Meyerhof & Adams, 1968; Davie & Sutherland, 1977; Rowe & Davis, 1982). Rowe & Davis (1982) noted that because of this cracking their analyses could not be used for shallow anchors. They did not provide alternative solutions for this situation.

The various mechanisms by which a rapidly loaded anchor may fail in uplift are depicted in Fig. 2. Figs 2(a) and 2(b) are for strips that separate from the soil beneath during loading, whereas Figs 2(c) and 2(d) are for anchors that have not separated from the soil beneath during loading.

Figure 2(a) shows a shallow anchor separated from the soil beneath. In this case the failure occurs as a result of shearing of the soil along lines directly above the edge of the strip (thus lifting the soil above the strip) and of tensile failure of the soil near the surface as a result of the 'beam' action.

Figure 2(b) shows the mechanism for a deep anchor separated from the soil beneath: in this case the mechanism of failure is shearing contained within the soil above the strip without surface effects. With the strip at great depth there is no significant surface expression, and hence the 'beam' action is absent.

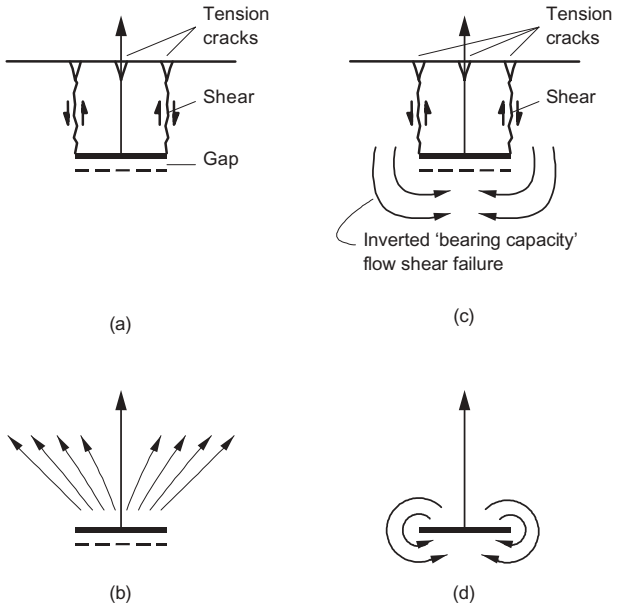

Fig. 2. Mechanisms of failure in uplift: (a) shallow anchor, separated from soil beneath; (b) shallow anchor, joined to soil beneath; (c) deep anchor, separated from soil beneath; (d) deep anchor, joined to soil beneath

Figure 2(c) shows the mechanism for a shallow anchor bonded with the soil beneath. In this instance the failure is by tension near the surface resulting from 'beam' action, shearing between the strip and these tensile cracks, and shearing beneath and beside the strip in a form of 'bearing capacity' failure as the soil beside the strip flows round to beneath the strip. As will be shown later, the self-weight of the soil is less important in this case.

Figure 2(d) shows the mechanism for a deep anchor bonded with the soil beneath. In this instance the soil flows around the strip, and the failure is in shear and is contained locally within the soil. It will be shown that, for this form of failure, the self-weight of the soil has no effect on the failure load.

Most of the published design methods show the value of either F or N_c as a function of H/B. At $H/B = 0$, the value of F or N_c is typically zero for the unbonded case or 5·14 for the bonded case, and increases to a maximum value of about 5·5–7·5 for the unbonded case as the anchor becomes buried. The corresponding values for the deeply buried bonded case are: for strips 11·42, i.e. $3\pi + 2$, as in Meyerhof (1951) and Rowe & Davis (1982); and, for circles, 12·42 and 13·11 for rough and smooth plates respectively (Martin & Randolph, 2001). Solutions for deep square, circular and rectangular anchors have also been published by Merifield *et al.* (2003). The value of H/B at which this maximum value is reached is called the *critical depth ratio*; it corresponds to the onset of the self-contained failure modes of Figs 2(b) and 2(d).

Forrest *et al.* (1995) and Das & Singh (1994) give the critical depth to diameter ratio for buried circular plates. Das (1978, 1980) provides estimates of the critical embedment ratio for square and circular plates, given by the embedment depth divided by the plate size (side length or diameter). In all these studies this critical depth ratio is given as a function of the shear strength alone. The former gives the critical depth to diameter ratio as about 1·2 for $c = 5$ kPa, increasing to about 3·5 at $c = 30$ kPa. The corresponding

values quoted by Das and Singh are 3 and 5·7. Das (1978) quotes values between 3 and 7 for circular and square plates over a similar range of strengths. For rectangular anchors Das (1980) indicates that the critical embedment ratio increases approximately linearly from the value for a square to a maximum of 1·55 times the value for a square when the plate has an aspect ratio of 3 or more. It must be kept in mind that Forrest *et al.* (1995) did not include overburden pressure in the expression for uplift capacity, whereas the papers by Das do include it.

These empirical relationships of critical depth to diameter ratio with soil strength are plotted in Fig. 3, together with data from other workers. The differences between the two curves for circular plates can be ascribed to different plate sizes and conditions, though both are from relatively small-scale experiments. It may be significant that Forrest *et al.* (1995) recommend that plate anchors should be installed to a depth of at least 5 diameters. It is also clear from Fig. 3 that neither curve is very reliable for other data.

It will be shown that the concept of a straight-line relationship up to a 'critical depth' is an oversimplification. In addition, the onset of the 'deep' failure load is shown to be a function of the size (either H or B), the soil density and the shear strength, plus the ability of the surface soil and the soil beneath the plate to accept tension.

Factors affecting separation

When uplift loading is applied, the (total) contact stresses beneath the plate decrease. With rapid loading this results in a decrease in the pressure in the pore fluid. Whether the strip will separate from the soil or not as a result depends on the physical conditions.

If the underside of the strip is connected to the outside air, or if the pore fluid cannot sustain tension, the strip will separate from the soil when the total stress reduction equals the initial total stress. Pores containing large proportions of air, or pore fluids with high dissolved gas contents, may be unable to sustain significant tension. This may be an important consideration for plate anchors embedded in some seabed soils, where gas contents, especially methane, may be significant.

If the soil is saturated, and the underside of the strip is open to water at the same hydrostatic level as the pore water, then separation will take place when the pressure reduction equals the initial effective overburden pressure.

In a saturated soil where the strip is sealed within the soil, separation cannot occur unless either:

(*a*) the pore pressures equalise by dissipation of the induced pore pressures, in which case an undrained analysis is invalid, as the loading is no longer 'rapid', or

(*b*) the pore pressure drops far enough below atmospheric for cavitation to occur—that is, failure in tension of the pore contents.

Estimates of the rate of dissipation of pore pressure around a plate can be made by the methods described in Booker & Small (1987) to test the assumption of undrained behaviour. Some other relevant information is also contained in Pyrah *et al.* (1985) and Small *et al.* (1998). A discussion of the effects of failure in tension of the pore contents is given below in the section 'Effect of allowable pore water pressure tension on uplift capacity'.

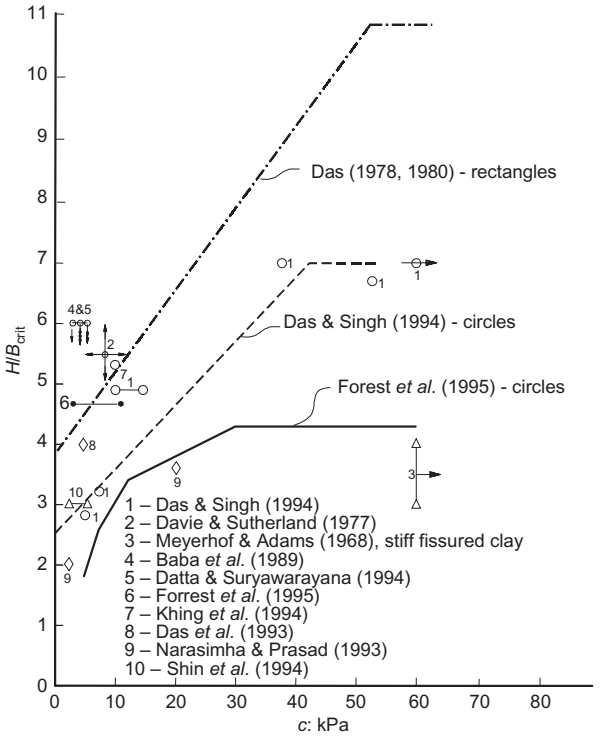

Fig. 3. Test data illustrating the effect of shear strength on the critical depth ratio for circular, square and rectangular anchors

Factors affecting soil tensile capacity near the soil surface

The concept of soil operating in tension is somewhat unusual. Finite element analyses in which tension was allowed showed a drop in total horizontal stress near the surface of approximately 100–160% of the shear strength. Although unsaturated soils can have some tensile strength in total stress terms, it is certainly not of this magnitude. Meyerhof & Adams (1968) indicated that tests on soft clays had given a tensile strength of 40% of the compressive strength but did not give any further details, and it is possible that this strength came from negative pore water pressures. Tests on unsaturated compacted clays gave tensile strengths in Brazilian tests of 25–78 kPa, and all the samples in these tests had unconfined compression strengths in excess of 500 kPa.

In saturated soils the presence of the pore water will allow some total stress tension to be sustained, and in a true undrained situation some tensile total stresses should be able to be accommodated. The tensile stresses caused by uplift of a strip are, however, right at the surface, and any negative pore water pressures could dissipate almost instantaneously provided there is free water at the surface. As a crack forms, only the soil at the very tip would need to drain for the crack to propagate. Such dissipation would occur at many orders of magnitude greater than dissipation for the pore pressures in the soil beneath and around the strip, and the view has been taken that pore pressures at the base of a crack from the surface will not drop below initial (hydrostatic) values.

ANALYSES UNDERTAKEN

Analyses of strip anchors in clay subjected to undrained uplift loading were undertaken using the finite element program AFENA (Carter & Balaam, 1995). The analyses assumed a thin, perfectly rigid strip, progressively displaced until failure occurred. Large-strain analyses were undertaken with re-meshing using an automatic mesh generation program developed by Hu & Randolph (1998). Most of the analyses were carried out assuming a smooth plate. Some check analyses with rough plates showed that the differences

were very minor. Two different soil models were used in this study.

In the first model, the soil was represented as a single-phase material, characterised by a shear strength, a tensile strength, Poisson's ratio, shear modulus and density (unit weight). In these analyses the tensile strength was taken as either very large or zero. For the analyses with zero tensile strength, if the minor principal (total) stress reduced to zero, the stresses at that Gauss point were maintained at that same value for all subsequent steps in the non-linear analysis. Poisson's ratio was always 0·49 to approximate constant-volume deformation and the ratio of shear modulus to shear strength (G/c) was 67, except for some analyses that were undertaken to examine the effect of changing this ratio.

In the second model, the soil was represented as a two-phase material. One phase was the soil skeleton, characterised by a shear strength, a tensile effective strength, effective Poisson's ratio, shear modulus and total density (unit weight). The second phase was the pore water, characterised by a very large bulk modulus, zero shear strength and stiffness, and with a limiting value for the negative pore pressure allowable. General details of the two-phase method can be found in some textbooks (e.g. Naylor *et al.*, 1981). In these analyses the soil tensile strength (measured in terms of effective stress) was taken as zero, and soil tension was dealt with in the same manner as for the single-phase soil. Various values were assigned to the limiting negative pore pressure. For the pore fluid, if the pore pressure dropped below a value of $-u_c$, the pore pressure was maintained at that value and the bulk stiffness was set to zero. The formulation can handle effective stress soil strength parameters, but, for the purpose of this work, a uniform strength was required, and so the artifice was used of giving the soil a cohesion only. The ratio of shear modulus to shear strength was kept as 67, as for the single-phase soil. Poisson's ratio of the solid skeleton was taken as 0·25, and for most analyses the total unit weight of the soil was taken as 20 kN/m^3 and the unit weight of the water was taken as 10 kN/m^3.

Both methods allow failure of the soil in tension. If the minor principal stress drops to zero the soil stresses are frozen and any requirement for zero volume change ceases, even in the two-phase soil. This is not strictly correct, because the major principal stress could theoretically continue to increase after tensile failure to $2c$ (or perhaps even larger if a truly frictional soil model had been assumed). This is likely to result in some underestimate of the capacity of shallow anchors with low values of $\gamma H/c$.

In the two-phase soil, if the pore water pressure reduces to below $-u_c$ then the no volume condition ceases and any further stress changes are transferred to the soil skeleton and the pore pressure is kept at $-u_c$.

Results of analyses are presented for the following cases.

1. Single-phase soil model, total stress tension allowed in all soil elements and tension allowed at the interface between the soil and the underside of the strip anchor.
2. Single-phase soil model, total stress tension allowed in all soil elements but with a no-tension joint immediately beneath the strip anchor.
3. Single-phase soil model with no total stress tension allowed anywhere in the soil.
4. Two-phase soil model with soil tensile failure if the minor principal effective stress reduces to zero. Above the strip no reduction in pore pressure below the initial pore pressure is allowed, whereas below the strip the total pore pressure is not allowed to reduce below zero (i.e. cavitation limit, $u_c = 0$).
5. Two-phase model with the soil above the strip as for Case 4 but with no cavitation limit for the soil beneath the strip (i.e. u_c large).
6. As for Case 5 but with varying cavitation limits.

Cases 1 and 2 do not have much physical validity, if any, but are included to allow comparison with other results and to demonstrate the effect of tensile failure on uplift capacity.

Analyses for case 1 using small-strain theory showed that the uplift capacity factor was independent of the soil strength, normalised as $\gamma H/c$. Large-strain analyses were also undertaken to assess the extent to which work done against gravity might influence results. Figure 4 shows the results of comparing large- and small-strain load deflection curves for a relatively shallow anchor ($H/B = 1$). For anchors with $H/B > 2$ the differences were negligible. Even for shallow anchors it was concluded that, although for very weak soils the large-strain results showed higher capacities, these higher capacities occurred at very large deformations, and for practical deformations the small-strain result was considered acceptable. Likewise, for high-strength soils, slightly lower capacities were recorded for very shallow anchors, but the difference was only 8% in the worst case. Large-strain analyses for case 2, which assumes no bonding between the underside of the strip and the soil, but allows tension in the soil itself, also showed similar differences between large- and small-strain answers, and also showed that the small-strain results were acceptable. The large-strain results did highlight the brittle nature of failure in higher-strength soils.

These results also showed that the inclusion of a density term in the expression for ultimate capacity, as in equation (1), is not required, and that equation (3) is more appropriate for expressing the anchor capacity. The results of case 2 showed that if $\gamma H/c < 7$, the mechanisms of failure were similar to Figs 2(a) and 2(b), whereas for greater values of $\gamma H/c$ the behaviour was identical to that of a fully bonded anchor.

The results of other cases are dealt with in later sections.

APPLICABILITY OF ANALYSES TO FIELD SITUATIONS

Unsaturated soils

Many applications of buried anchors involve unsaturated soils, including transmission tower anchors and the like. In most instances these will be buried in compacted clays, because of the difficulty of installing a horizontal anchor plate in undisturbed soil. Because of the air in the pore fluid, it is reasonable to assume that the soil near the surface will fail in tension if the total stress drops below zero. Beneath

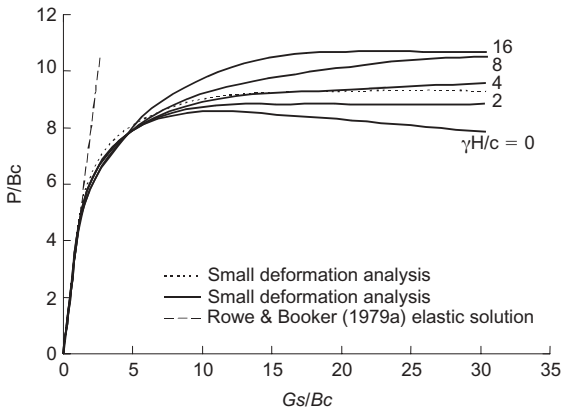

Fig. 4. Load–deflection curves for large and small deformation analyses of fully bonded, tension allowed soil (case 1), $H/B = 1$

the plate the soil and plate would part if the total stress dropped below zero, though the extent will depend on the proportion of air and the speed with which air can get access to the underside of the strip. Unless other information is available, for example the results of full-scale tests at the same site, a reasonable approach is to assume that no total stress tension can be tolerated beneath the plate. Thus the analyses of case 3 (the single-phase soil no-tension analysis) would be adopted.

Caution needs to be exercised if the surface is exposed, as drying tension cracks could reduce the uplift capacity.

Saturated soil

In saturated soils, separation will occur only if the effective stress beneath the plate drops below zero. This can occur only if the negative pore pressures beneath the plate dissipate (unless cavitation occurs; see below). If dissipation occurs then the surrounding soil will also have drained, and the undrained analysis solutions are no longer applicable. On the other hand, dissipation of the negative pore pressures in the tensile zone near the surface could occur much more rapidly, as discussed above.

It is therefore concluded that for design in such circumstances the results for case 5 (the two-phase soil, large u_c analysis) should be used. It is also necessary to check for cavitation. In deep water and weak soils this will not be a problem, but in other cases a check should be made using the methods described subsequently in the section 'Effect of allowable pore water tension on uplift capacity'.

RESULTS FOR ANCHORS IN A SINGLE-PHASE SOIL (CASE 3)

The distributions of shear and tensile failure in the soil are shown in Figs 5(a)–5(d). Figures 5(a) and 5(b) show results for relatively shallow anchors with $H/B = 1$. Figure 5(a) is for a relatively strong soil, $\gamma H/c = 1$, whereas Fig. 5(b) is for $\gamma H/c = 8$, which approximates a normally consolidated soil. It can be seen that, for the strong soil, the

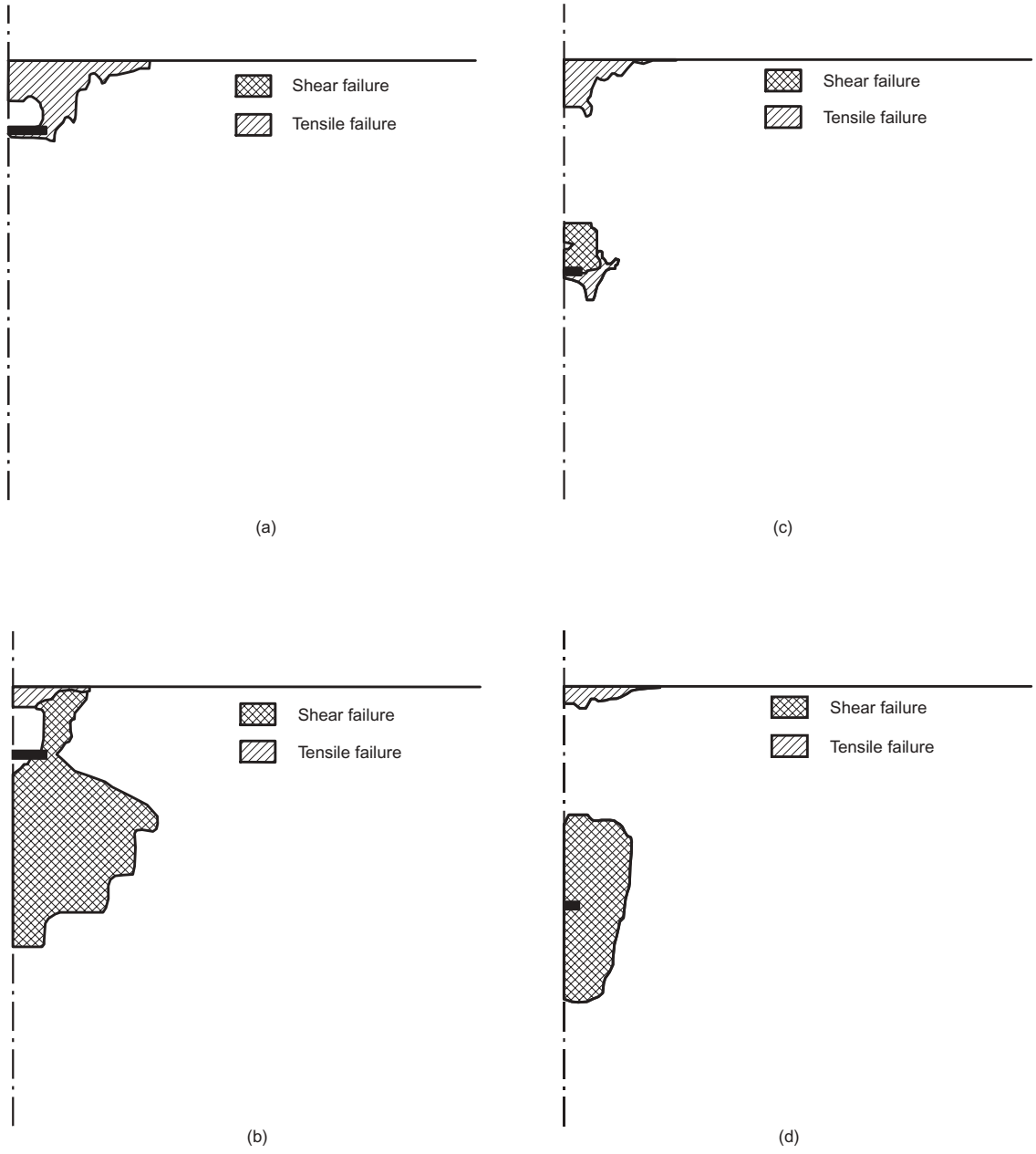

Fig. 5. Typical failure zones predicted by single-phase, no-tension analysis (case 3): (a) $H/B = 1$, $\gamma H/c = 1$; (b) $H/B = 1$, $\gamma H/c = 8$; (c) $H/B = 6$, $\gamma H/c = 1$; (d) $H/B = 6$, $\gamma H/c = 8$

tensile stresses near the surface cause failure from the surface to the plate. Thus the failure is all tensile, and the plate separates, whereas for the normally consolidated soil separation does not occur, and the failure is mostly in shear, although there is some tensile failure near the surface.

Figures 5(c) and 5(d) show deep strips with $H/B = 6$, again for the same two values of $\gamma H/c$. In these relatively deep anchors tensile failure still occurs at the surface but does not join the failed sections around the strip. For the relatively strong soil the strip separates from the soil beneath: tensile failure or splitting occurs next to the strip, and shear failure occurs above the strip. In the normally consolidated soil only shear failure is predicted to occur near and immediately above the strip.

These figures demonstrate the importance of the two non-dimensional parameters H/B and $\gamma H/c$ in determining the way that failure occurs and hence the load deflection and ultimate load behaviour. It was found that the relative stiffness (or 'rigidity index'), G/c, did not affect the anchor plate behaviour to any significant degree; this ratio was 67 and Poisson's ratio was 0·49 for all results given in this section.

The ultimate values for the uplift parameter N_c are shown in Fig. 6 as a function of H/B for various values of $\gamma H/c$. Also included are the values for the tension-allowed analysis with a no-tension joint beneath the strip (case 2). As tensile failure is included beneath the anchor for both cases, the differences between the two sets of curves are caused by the tensile failure near the soil surface. The percentage reduction in ultimate capacity resulting from tensile failure above the strip depends on $\gamma H/c$, and for most values of H/B ranges typically from 30% at $\gamma H/c = 1$ to less than 10% when $\gamma H/c = 3$ and to less than 5% when $\gamma H/c$ is 6 or more.

The capacity of the soil above the strip to accept a reduction in horizontal stress is also dependent on the initial in-situ value of the ratio of total horizontal and total vertical stresses, denoted here as K_t. Clearly a large value of K_t results in higher initial horizontal stresses and hence a greater capacity to accept horizontal stress reductions before the stresses become tensile. A greater value of K_t gives higher capacity: for example, in the cases where $K_t = 1$ and 0·9, the uplift capacity factors for anchors with $H/B = 1$ and $\gamma H/c = 4$ are 5·61 and 5·55 respectively. The factors shown in Fig. 6 are for $K_t = 1$.

The nature of the load–deflection curve to failure is also dependent on H/B and $\gamma H/c$. Fig. 7 shows some typical non-dimensional load–deflection curves presented as P/Bc against Gs/Bc, where s is the strip deflection and P is the applied force. Rowe & Booker (1979) give a method of calculating the elastic deflections, and these are also shown in Fig. 7. It is convenient to give the deflection to failure as a ratio K of the deflection at failure to the deflection that would occur if the soil had remained elastic up to that load. Table 1 shows the results for a range of values of H/B and $\gamma H/c$. It should be noted that, with strong soils ($\gamma H/c = 1$), sudden failure occurs at relatively low deflections. For shallow anchors in weak soils ($\gamma H/c \geqslant 8$), very large deflections may be required to attain the ultimate load, as is also the case for deep anchors of intermediate strength ($2 < \gamma H/c < 4$).

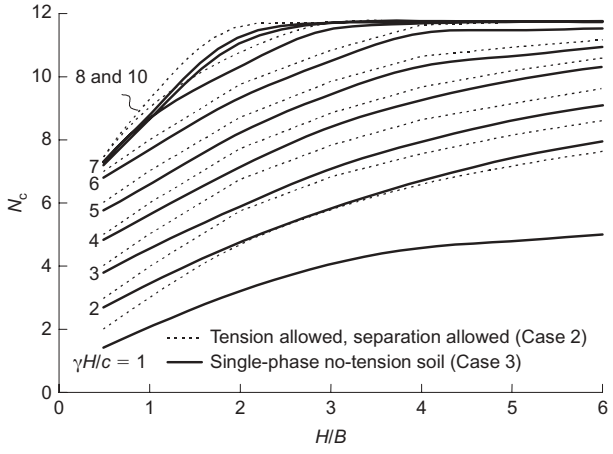

Fig. 6. Uplift capacity against H/B for single-phase, no-tension soil (case 3) compared with tension-allowed soil with separation (case 2)

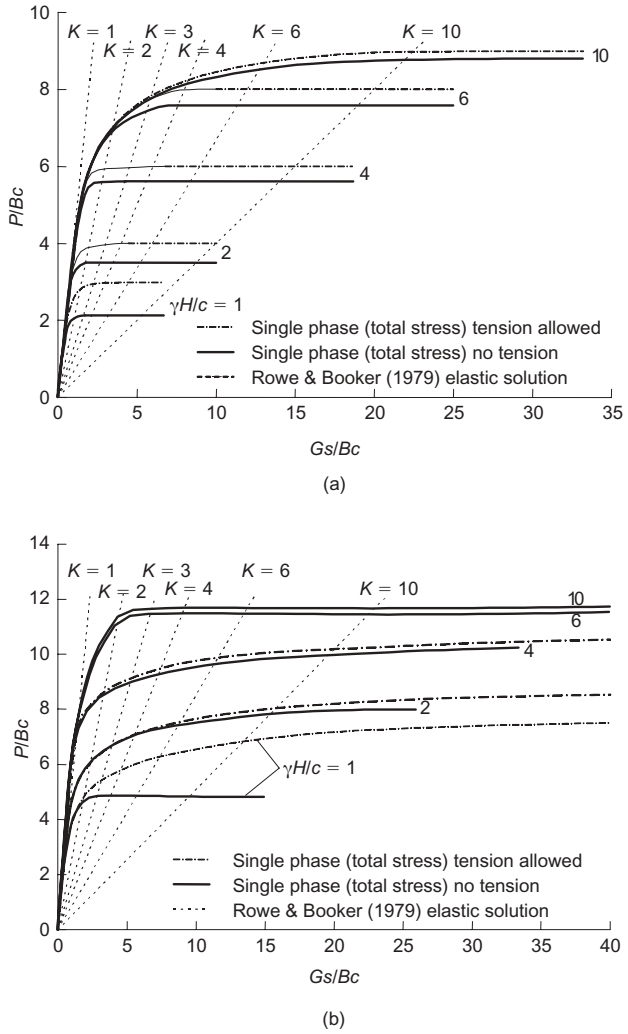

Fig. 7. Load–displacement curves predicted by single-phase, no-tension analysis (case 3): (a) $H/B = 1$; (b) $H/B = 6$

The distribution of pressure across the strip is important for the design of real anchors. The distribution of load across the strip is shown in Fig. 8 in non-dimensional form as net vertical pressure normalised by the stress quantity (P/B). Figure 8(a) is for loads of one-third the ultimate, and all the curves are very similar, with significant stress concentrations near the edge. This is an important consideration in the structural design of an anchor, because most anchors will work in this range of loading. By contrast, Fig. 8(b) shows the distribution at failure. In this case, the distribution is relatively uniform except for the case of a shallow anchor ($H/B = 1$ in strong soil, $\gamma H/c = 1$). Fig. 8(c) shows the reduction in stress beneath the anchor at failure for cases where the anchor does not separate. It will be seen that in both cases the reduction is from 6 to 7 times the shear

Table 1. Failure deflection ratio, *K*, predicted by single-phase analyses

$\gamma H/c$	Tension allowed above plate (case 2)			No tension (case 3)		
	$H/B = 1$	$H/B = 3$	$H/B = 6$	$H/B = 1$	$H/B = 3$	$H/B = 6$
1	4	7	16	3	3	3
2	4	6·5	14	3	4	10
4	4	6	10	3	5	9
6	5	6	4	4	5	3
8	8	5·5	3	7·5	5	3
10	10	5	3	10	5	3

strength. This is similar to the value noted in Rowe & Davis (1982).

RESULTS FOR ANCHORS IN A TWO-PHASE SOIL (CASES 4 AND 5)

As noted above, the analyses for cases 4 and 5 used a two-phase soil model. All calculations assumed that Poisson's ratio of the soil skeleton was 0·25, $K_0 = 1{\cdot}0$, the total unit weight of soil was 20 kN/m^3, and the unit weight of pore water was 10 kN/m^3. The calculations are not especially sensitive to Poisson's ratio but are affected by K_0 and the density insofar as they affect the initial horizontal effective stress. Common to both cases is the assumption that pore pressure dissipation at the base of a crack starting from the surface will be virtually instantaneous, and so tensile failure will occur when the reduction in horizontal stress equals the initial horizontal effective stress for the material above the strip.

Below the strip in case 4 it is assumed that the pore water cannot accept any negative pressure. This means that the strip will separate from the underlying soil when the total stress reduction beneath the strip equals the initial total vertical stress. In practice this is the same assumption as was made for the soil model for case 3. Below the strip in case 5 it is assumed that the pore water can sustain any negative pore pressures without failure. In practice this means that the strip always stays in contact with the soil beneath it.

The mechanisms of failure for case 4 are very similar to those shown in Fig. 5, although the change from tensile to shear failure above the strip occurs at higher values of $\gamma H/c$. Likewise, the mechanisms of failure for case 5 always show shear failure beneath the strip but show similar mechanisms to case 4 above the strip.

Figure 9 shows the ultimate uplift values obtained for cases 4 and 5. It will be seen that, once $\gamma H/c$ exceeds 6 to 8, there is little difference between the two predictions. This is because the value of the total vertical stress change below the anchor required to cause shear failure adjacent to and below the anchor is less than the initial total vertical stress, so tension does not occur beneath the anchor. At smaller values of $\gamma H/c$ the capacities for case 4 are substantially below those for case 5. An interpolation method to deal with different values of the allowable negative pore pressure, u_c, is given in the next section.

It is instructive to compare the ultimate values of P/Bc for case 3 with those for case 4. In effect, in the former case the clay fails in horizontal tension above the plate when the horizontal stress reduction is the same as the total overburden pressure, whereas in the latter case the clay experiences failure at half this total stress reduction. This is also analogous to using the case 3 analysis with a K_t of 0·5 instead of 1·0. The effect where $\gamma H/c = 1$ (strong soil) is to reduce the ultimate load by about 30% at $H/B < 4$, reducing to 14% at $H/B = 6$. The reduction is under 10% where $\gamma H/c > 3$.

The distribution of load across the strip is shown in Fig. 10 in non-dimensional form as net vertical total pressure normalised by P/B. Figure 10(a) is for loads of one-third the ultimate, and all the curves are very similar, with significant stress concentrations near the edge. By contrast, Fig. 10(b) shows the distribution at failure. In this case the load is relatively uniform except for the case of a shallow anchor ($H/B = 1$) in strong soil ($\gamma H/c = 1$). Figure 10(c) shows the reduction in total stress beneath the anchor at failure where the anchor does not separate. It will be seen that in both cases the reduction is from 6 to 7 times the shear strength. All these distributions are very similar to those for the single-phase soil (Fig. 8).

The nature of the load–deflection curves for the two-phase soil is similar to those for the single-phase soil. Table 2 shows the values of K at failure—that is, the ratio of the deflection at failure to that which would occur at that load if the soil remained elastic. It should be noted that, with strong soils ($\gamma H/c = 1$), sudden failure occurs at relatively low deflections. For shallow anchors in weak soils ($\gamma H/c \geqslant 8$), very large deflections may be required to attain the ultimate load, as is also the case for deep anchors of intermediate strength ($\gamma H/c = 4$).

EFFECT OF ALLOWABLE PORE WATER TENSION ON UPLIFT CAPACITY

For pure water at normal temperatures (5–25°C) cavitation (boiling) will occur at a pressure of 80–95 kPa below atmospheric. In clay soils, it is known that the water bound within the clay platelets can withstand much higher negative pressures. It is unlikely, however, that this would apply to the free water in the voids within the soil, and although more research is required to ascertain the actual behaviour, it is considered prudent to assume that pore water would also cavitate at pressures similar to normal water. The stress distributions in Figs 8(c) and 10(c) show that where separation does not occur the reduction in total stress below the strip is of the order of seven times the undrained shear strength. Thus cavitation can occur if the tolerable pore tension plus the initial pore pressure plus the initial effective vertical stress is less than seven times the undrained shear strength. In stiff soils this can occur, and it will be necessary to use a lower capacity if

$$7c > \gamma' H + u_0 + u_c \tag{4}$$

where u_0 is the initial pore pressure above atmospheric (kPa), u_c is the (absolute) magnitude of the pressure drop below atmospheric at which water will cavitate (kPa), and γ' is the submerged unit weight of the soil (kN/m^3).

If $(\gamma' H + u_0 + u_c) < 7S_u$ then the capacity will be intermediate between case 4 and case 5. Based on the analyses presented in the previous section, the reduced capacity caused by cavitation can either be approximated directly

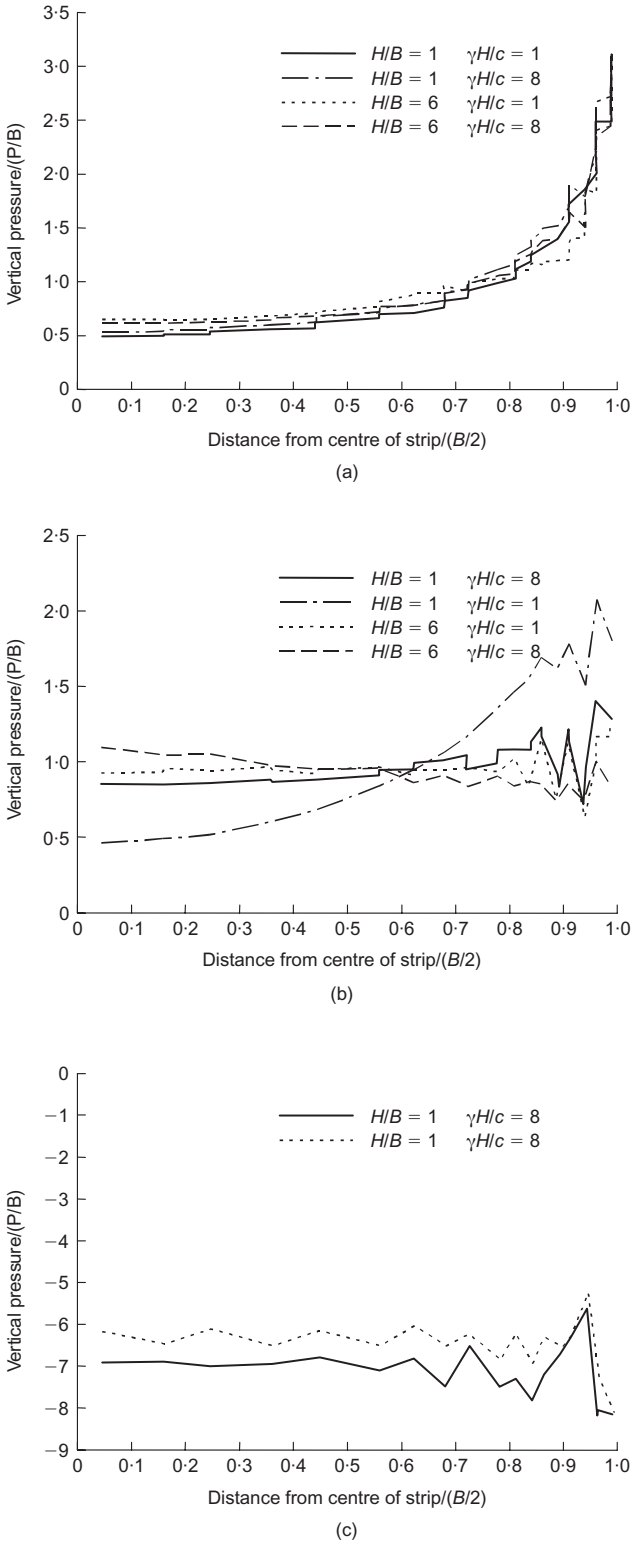

Fig. 8. Normalised stress distributions across the strip (case 3): (a) one-third ultimate load; (b) ultimate load; (c) net total stress change beneath strip

from the values given or, for other cases, this reduced capacity could be taken as

$$P_{ult} = P_4 + (P_5 - P_4)\left(\frac{u_0 + u_c - \gamma_w H}{7c - \gamma H}\right) \quad (5)$$

where P_4 is the uplift capacity for case 4, and P_5 is the uplift capacity for case 5.

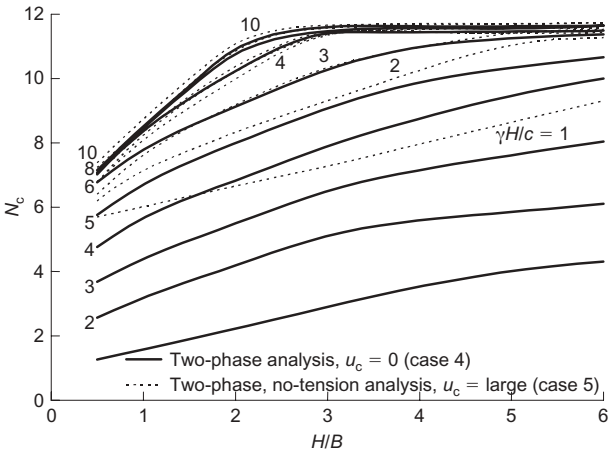

Fig. 9. Uplift capacity for no-tension, two-phase soil, $u_c = 0$ (case 4) and u_c = large (case 5)

Equation (5) becomes unstable near the point where γH approaches $7c$, as both the numerator and denominator in this equation approach zero, so some judgement is required.

Figure 11 shows a comparison of the results of finite element analyses as compared with the approximate predictions of equation (5). It can be seen that generally good agreement is obtained.

COMPARISON WITH EXPERIMENTAL RESULTS

Most of the experimental data in the literature are for the uplift of circular or square plates. Two sets of data for strips were found. Rowe & Davis (1982) described experiments on 6 mm brass strips, 13–38 mm wide and 64–190 mm long. They indicated that there was little change in results once the aspect ratio (L/B) exceeded 5, and that results for lower aspect ratios were slightly larger. The soil was a kaolin clay and was consolidated with an overburden pressure of 200 kPa before unloading and testing, resulting in an average undrained shear strength of 50 kPa. Because of this preparation there would have been considerable initial horizontal pressures in the soil at the time of testing. Tension cracks were noted at H/B values of less than 2·5. Figure 12 shows a comparison of calculations, made assuming an allowable reduction in horizontal stress at the surface of 50 kPa, with the experimental results. The test results are shown in Fig. 12 compared with calculations assuming that (1) the soil can take unlimited tension, and (2) the soil can sustain a 50 kPa reduction in horizontal stress. This latter series showed only very small tension cracks for $H/B = 3$ or more. It will be seen that the test results lie reasonably on the second line for shallow strips but nearer the first for higher values of H/B. It is noted that in the paper the opinion was given that the rods attached to the strip to apply the uplift loading accentuated the surface cracking.

Khing *et al.* (1994) reported results for a buried strip, 76 mm wide by 152 mm long and 13 mm thick, buried in clay with a liquid limit of 43%, placed in a relatively wet condition to give an average shear strength of 10·2 kPa. The strip was sat on top of a Plexiglas box to prevent any contribution to the capacity by underlying soil. The soil was kneaded into place to exclude air bubbles. This placement method would have resulted in continual passive failure in the clay, with the result that the initial horizontal stress was close to twice the undrained shear strength. With such a high initial horizontal stress, tensile failure at the surface would not be expected. Figure 13 shows the experimental results together with those for calculations allowing tension

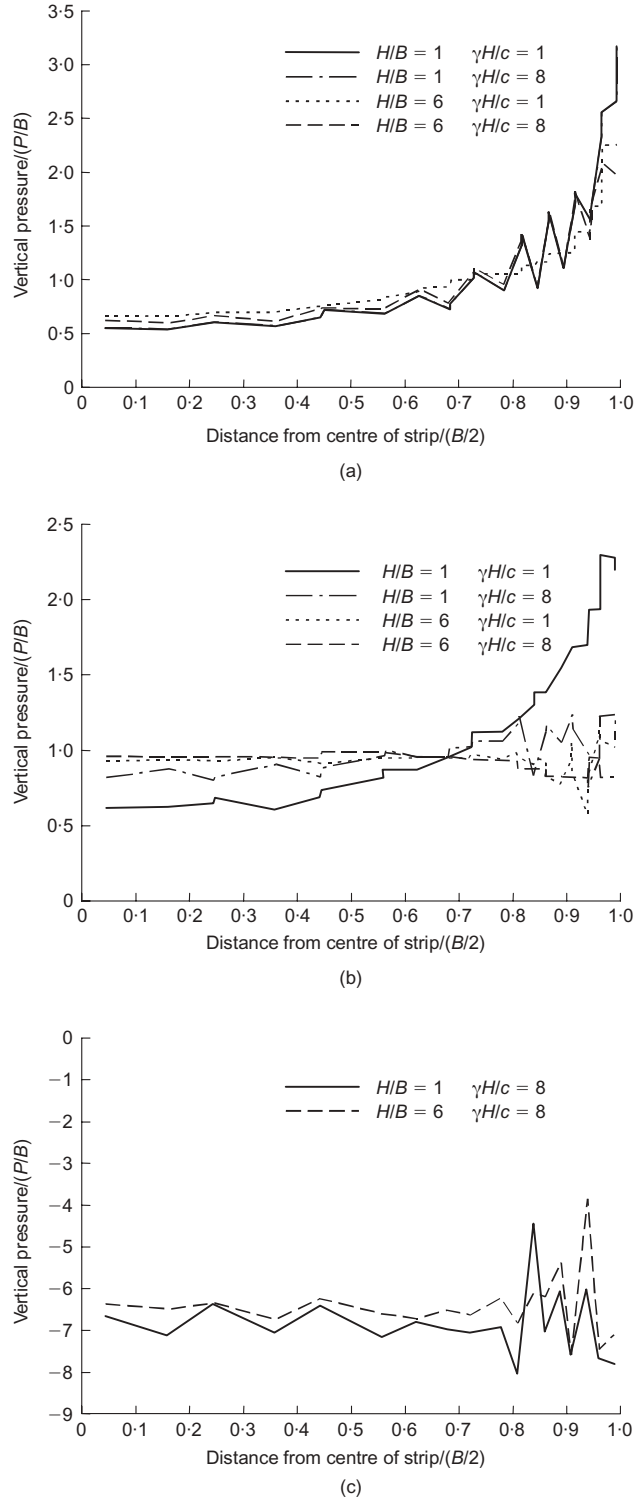

Fig. 10. Normalised stress distributions across the strip (case 4): (a) one-third ultimate load; (b) ultimate load; (c) net total stress change beneath strip

to develop in the soil and plate separation (case 2), and there is reasonable agreement, although the experimental results are rather higher, as might be expected given their relatively low aspect ratio. The box beneath the strip would tend to inhibit failure at greater H/B values because the soil could not move around to beneath the strip so readily.

CONCLUSIONS

(*a*) The analyses described in this paper show that the behaviour of strips in uplift is a function of the non-dimensional parameters H/B, $\gamma H/c$ and u_c/c. These represent the effects of depth of burial, the relative effects of overburden pressure and shear strength, and the capacity of the pore fluid to accept tension. At normal temperatures water can accept pressures in the region of 80–95 kPa below atmospheric without vaporising. It is probable that this will also apply to water in macropores within a saturated soil, although more research is required to investigate this behaviour. Gas in solution could also limit the effective value of u_c.

(*b*) The ultimate uplift capacity is dependent also on the availability of water at the soil surface and beneath the strip. Some guidelines for this are provided in the section 'Applicability of analyses to field situations', and in the discussion on separation in the subsection 'Factors affecting separation'. Designers need to consider the particular circumstances of their problem.

(*c*) In shallow anchors, failure in tension occurs from the surface downwards. The stronger the soil, the more likely is tensile failure, and the deeper the strip has to be before tensile failure does not occur.

(*d*) When anchors are deeply buried the failure pattern is a localised shear failure around the anchor, and the capacity becomes a function only of shear strength and is independent of the overburden pressure.

(*e*) The deflection at failure is very variable, as shown in Tables 1 and 2. In stronger soils, tensile failure results in low deflections at ultimate collapse, and overload could result in sudden failure. By contrast, for shallow anchors in weaker soils, the deflection to failure can be very high, and if deflections need to be limited, conservative factors of safety are required.

(*f*) Intuitively, it should be expected that the capacity of shallow anchors will be significantly affected by the magnitude of horizontal stresses prior to anchor loading. The limited results presented in this study confirm this expectation. In compacted clay fills high horizontal stresses commonly exist after placement, and can be as high as $2c$. These may dissipate with time as the surrounding soil creeps away or as drying induces tension cracks in adjacent soil. Care is therefore necessary in interpreting the results of field tests on shallow anchors.

(*g*) The curves given in Figs 6 and 9 were computed for $\gamma = 20\ \text{kN/m}^3$ and $\gamma_w = 10\ \text{kN/m}^3$ and for $K_t = 1$. The

Table 2. Failure deflection ratio, *K*, predicted by two-phase, no-tension analyses

$\gamma H/c$	$u_c = 0$ (case 4)			u_c = large (case 5)		
	$H/B = 1$	$H/B = 3$	$H/B = 6$	$H/B = 1$	$H/B = 3$	$H/B = 6$
1	2	3	3·5	5	4	3·5
2	3	4	4	6	4·5	3·5
4	3·5	5	12	8	7	3·5
6	5·5	5	5	9	7	3·5
8	10	5	3·5	10	7·5	3·5
10	10	5	3·5	12	7·5	3·5

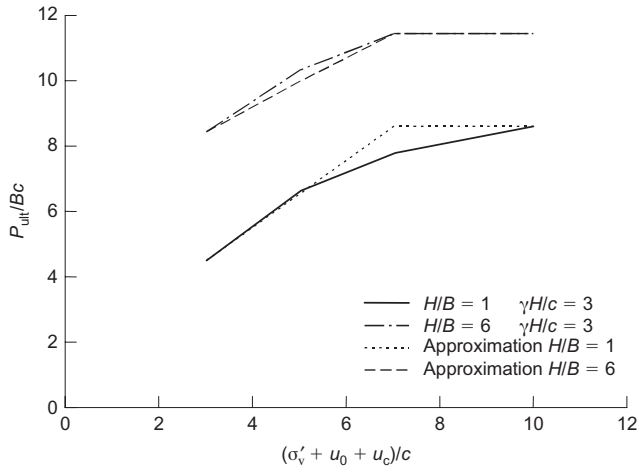

Fig. 11. Effect of the ability of the pore water to accept negative values on the uplift capacity, and comparison with predictions of equation (5)

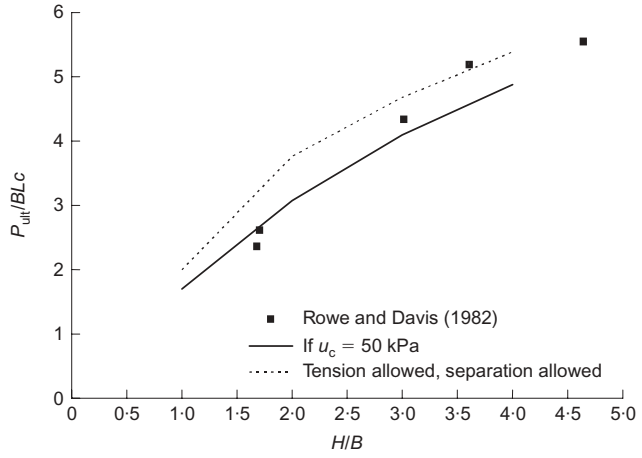

Fig. 12. Comparison of calculated values and experimental results from Rowe & Davis (1982)

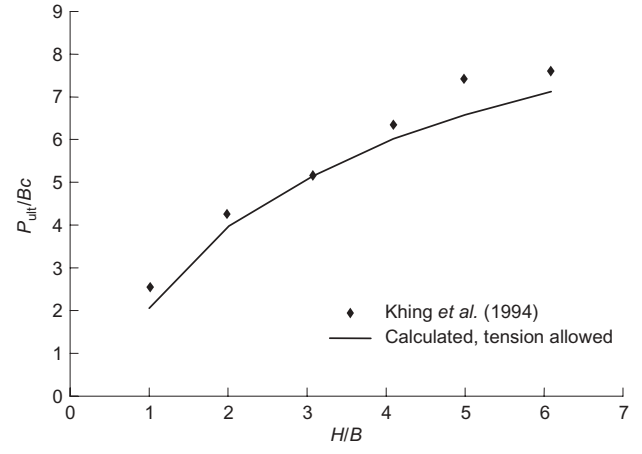

Fig. 13. Comparison of calculated values and experimental results from Khing *et al.* (1994)

effect of changing the soil density is simply reflected in the corresponding change in the parameter $\gamma H/c$. In situations where horizontal tensile failure occurs in the soil, the ultimate uplift capacity is likely to be sensitive to K_t.

(*h*) The predictions presented here indicate that reductions in the uplift capacity can be as much as 30% due to tensile failure of the soil (Fig. 6). This effect is most pronounced for anchors characterised by low values of the parameter $\gamma H/c$.

(*i*) Model tests in normal gravity have very low values of $\gamma H/c$. In addition, many preparation techniques cause high initial horizontal stresses. Account must be taken of these factors when applying the results of such tests to full-scale design.

(*j*) In the normal working range of loading, there is a significant load concentration near the edge of the strip, and this needs to be taken into account in the structural design of strip anchors.

ACKNOWLEDGEMENTS

Some of the work described here forms part of the research programme of the Special Research Centre for Offshore Foundation Systems, established and supported under the Australian Research Council's Research Centres Programme. In addition, a Large Grant from the Australian Research Council to investigate the finite deformation behaviour of soils is also gratefully acknowledged.

NOTATION

B width of strip anchor plate
c shear strength of soil
G shear modulus of soil
H depth from surface of strip anchor plate
K ratio of deflection at failure to that corresponding to elastic deflection at same load
L length of plate
N_c uplift capacity factor for a strip anchor
P force on anchor in uplift
P_{ult} ultimate force on anchor in uplift
P_4 maximum value of P_{ult} for case 4
P_5 maximum value of P_{ult} for case 5
s deflection of plate
u_0 initial pore pressure at plate
u_c maximum drop below atmospheric pressure that pore fluid can accommodate
γ bulk unit weight of soil
γ' submerged unit weight of soil

REFERENCES

Baba, H. U., Gulhati, S. K. & Datta, M. (1989). Suction effect in plate anchors in soft clays. *Proc. 12th Int. Conf. Soil Mech. Found. Engng, Rio de Janeiro* **1**, 409–412.

Booker, J. R. & Small, J. S. (1987). The time deflection behaviour of a rigid under-reamed anchor in a deep clay layer. *Int. J. Numer. Anal. Methods Geomech.* **11**, 269–281.

Carter, J. P. & Balaam, N. P. (1995). *AFENA: Users' manual*. Centre for Geotechnical Research, Department of Civil Engineering, University of Sydney, Australia

Das, B. M. (1978). Model tests for uplift capacity of foundations in clay. *Soils Found.* **18**, No. 2, 17–24.

Das, B. M. (1980). A procedure for estimation of ultimate capacity of foundations in clay. *Soils Found.* **20**, No. 1, 77–82.

Das, B. M. & Singh, G. (1994). Uplift capacity of plate anchors in clay. *Proc. 4th Int. Offshore and Polar Engineering Conf., Osaka* **1**, 436–442.

Das, R. N., Shin, E. C., Das, B. M., Puri, V. K. & Yen, S. C. (1993). Creep of plate anchors in clay. *Proc. 3rd Int. Offshore and Polar Engineering Conf., Singapore* **1**, 538–543.

Davie, J. R. & Sutherland, H. B. (1977). Uplift resistance of cohesive soils. *J. Geotech. Div., ASCE* **103**, No. GT9, 935–952.

Datta, M. & Suryanarayana, C. V. (1994). Elimination of suction beneath plate anchors in model tests: a comparison of two methods. *Proc. 4th Int. Offshore and Polar Engineering Conf., Osaka* **1**, 456–459.

Forrest, J., Taylor, R. & Bowman, L. (1995). *Design guide for pile-driven plate anchors*, Technical Report TR-2039-OCN, Port Hueneme, CA: Naval Facilities Research Center.

Hu, Y. & Randolph, M. F. (1998). A practical numerical approach for large deformation problems in soil. *Int. J. Numer. Anal. Methods Geomech.* **22**, 327–350 (see also Research Report G1226, Department of Civil Engineering, University of Western Australia, 1996).

Khing, K. H., Das, B. M. & Yen, S. C. (1994). Uplift capacity of strip plate anchors in clay with sloping surface. *Proc. 4th International Polar and Offshore Engineering Conf., Osaka* **1**, 467–471.

Martin, C. M. & Randolph, M. F. (2001). Applications of lower and upper bound theorems of plasticity to collapse of circular foundations. *Proc. 10th Int. Conf. on Computer Methods and Advances in Geomechanics, Tucson* **2**, 1417–1428.

Merifield, R. S., Sloan, S. W. & Yu, H. S. (1999). *Stability of plate anchors in undrained clay*, Research Report No. 174·02·1999. University of Newcastle, Australia.

Merifield, R. S., Sloan, S. W. & Yu, H. S. (2001). Stability of plate anchors in undrained clay, *Géotechnique* **51**, No. 2, 141–153.

Merifield, R. S., Lyamin, A. V., Sloan, S. W. & Yu, H. S. (2003). Three-dimensional stability analysis of plate anchors in clay, *J. Geotech. Geoenviron. Engng, ASCE* **29**, No. 3, 243–253.

Meyerhof, G. G. (1951). The ultimate bearing capacity of foundations. *Géotechnique* **2**, No. 4, 301–332.

Meyerhof, G. G. & Adams, J. I. (1968). The ultimate uplift of foundations. *Can. Geotech. J.* **5**, No. 4, 225–244.

Narasimha, S. & Prasad, Y. V. S. N. (1993). Experimental studies on plate anchors in layered marine soils. *Proc. 3rd Polar and Offshore Engineering Conf., Singapore* **1**, 544–550.

Naylor, D. J., Pande, G. N., Simpson, B. & Tabb, R. (1981). *Finite elements in geotechnical engineering*, pp. 29–34. Swansea: Pineridge Press.

Pyrah, I. C., Hird, C. C. & Tanaka, Y. (1985). Consolidation behaviour of a single underream anchor. *Proc. 5th Int. Conf. on Numerical Methods in Geomechanics, Nagoya*, 629–636.

Rowe, R. K. & Booker, J. R. (1979). A method of analysis for horizontally imbedded anchors in an elastic soil. *Int. J. Numer. Anal. Methods Geomech.* **3**, 187–203.

Rowe, R. K. & Davis, E. H. (1982). The behaviour of anchor plates in clay. *Géotechnique* **32**, No. 1, 9–23.

Shin, E. C., Das, R. N., Omar, M. T., Das, B. M. & Cook, E. E. (1994). Mud suction force in the uplift of plate anchors in clay. *Proc. 5th Int. Offshore and Polar Engineering Conf.*, The Hague, Netherlands, **1**, 462–466.

Small, J. S., Thorne, C. P. & Ta, L. (1998). Effect of pore pressure dissipation on the behaviour of plate anchors in clay. *Proc. 8th Int. Polar and Offshore Engineering Conf., Montreal*, 497–504.

Sutherland, H. B. (1988). Uplift resistance of soils. *Géotechnique* **38**, No. 1, 493–516.